Steel and Composite Structures, *Vol. 30, No. 3 (2019) 271-280*
DOI: https://doi.org/10.12989/scs.2019.30.3.271

Computational and experimental analysis of beam to column joints reinforced with CFRP plates

Zhenyan Luo [1], Hamid Sinaei [2], Zainah Ibrahim [2], Mahdi Shariati [2,3], Zamin Jumaat [2], Karzan Wakil [4], Binh Thai Pham [*5], Edy Tonnizam Mohamad [6] and Majid Khorami [7]

[1] *School of Resources and Safety Engineering, Central South University, Changsha, 410083, China*
[2] *Department of Civil Engineering, University of Malaya, 50603 Kuala Lumpur, Malaysia*
[3] *Faculty of Civil Engineering, University of Tabriz, Tabriz, Iran*
[4] *Research Center, Sulaimani Polytechnic University, Sulaimani 46001, Kurdistan Region, Iraq*
[5] *Institute of Research and Development, Duy Tan University, Da Nang 550000, Vietnam*
[6] *Centre of Tropical Geoengineering (GEOTROPIK), Faculty of Civil Engineering, Universiti Teknologi Malaysia, Johor Bahru, Malaysia*
[7] *Universidad UTE, Facultad de Arquitectura y Urbanismo, Calle Rumipamba s/n y Bourgeois, Quito, Ecuador*

(*Received April 8, 2018, Revised August 15, 2018, Accepted January 26, 2019*)

Abstract. In this paper, numerical and experimental assessments have been conducted in order to investigate the capability of using CFRP for the seismic capacity improvement and relocation of plastic hinge in reinforced concrete connections. Two scaled down exterior reinforced concrete beam to column connections have been used. These two connections from a strengthened moment frame have been tested under uniformly distributed load before and after optimization. The results of experimental tests have been used to verify the accuracy of numerical modeling using computational ABAQUS software. Application of FRP plate on the web of the beam in connections to improve its capacity is of interest in this paper. Several parametric studies were carried out for CFRP reinforced samples, with different lengths and thicknesses in order to relocate the plastic hinge away from the face of the column.

Keywords: CFRP plate; plastic hinge relocation; finite element; rehabilitation; strengthening

1. Introduction

Rehabilitation and strengthening of old or pre-damaged building structures and bridges made up of Reinforced Concrete (RC) are vexatious challenges for the structural design engineers (Shariati 2008, Hamidian *et al*. 2012, Liu *et al*. 2014). The replacement of deficient structures is not always possible due to high expenditures and usage limitations. Thus, the structures built several decades ago may need to be strengthened and upgraded to meet the current service load demands (Shahabi *et al*. 2016). Performing a strengthening and retrofitting program is more reasonable compared to the demolishing and rebuilding of structures when considering the disruption of services, labour and materials cost (Tang *et al*. 2006, Allahvirdizadeh *et al*. 2011, Hadi and Tran 2016). The required strength and serviceability performance of a strengthened structure could only be achieved through a complete understanding of the behaviour of the material and techniques used for strengthening purpose (Daly and Witarnawan 1997, Nordin 2005, McCormac and Brown 2015).

Several methods of strengthening RC structures using various materials have been studied and applied in the rehabilitation field (Khanouki *et al*. 2010, 2011, Daie *et al*. 2011, Sinaei *et al*. 2011, 2012, Jalali *et al*. 2012, Mohammadhassani *et al*. 2013a, b, 2014a, b, Khorami *et al*. 2017, Heydari and Shariati 2018, Shariat *et al*. 2018, Zandi *et al*. 2018). When it comes to the materials, the most recent type of the material utilized for strengthening purpose in modern era is Fibre Reinforced Polymer (FRP) composites (Joshi *et al*. 2014, Aslam *et al*. 2015, Joshaghani 2017). The advantages of FRP that supersede the traditional strengthening materials may said to be the sufficient opposition to rust, excellent strength as compared to the self-weight, user friendly and neutrality to electro-magnetic forces (Shafaei *et al*. 2016). All of these benefits strongly recommend to use the FRPs for the strengthening of RC structures; especially in the cases where traditional steel reinforcement fails to provide required serviceability (Aslam *et al*. 2015). Strengthening with FRP composites is one of the recent retrofitting and strengthening techniques (Engindeniz *et al*. 2005, Andalib *et al*. 2014).

The beam-to-column connections (BCCs) are the perilous region of RC framed structures intended to provide resistance to applied static or seismic load in plastic region (Momenzadeh *et al*. 2017). A poor frame design enhances the chances of creation of plastic hinge in the column that makes the column fail at lower ultimate load as well as reduce the energy dissipation capability of the column, which is dependent of axially applied load and design of reinforcement (Thomas and Priestley 1992). A way out of this problem is to design the ductile moment-resisting (DMR) frames based on strong-column-weak-beam design.

∗Corresponding author, Ph.D.,
E-mail: phambinhgtvt@gmail.com

http://www.techno-press.org/?journal=scs&subpage=6
ISSN: 1229-9367 (Print), 1598-6233 (Online)

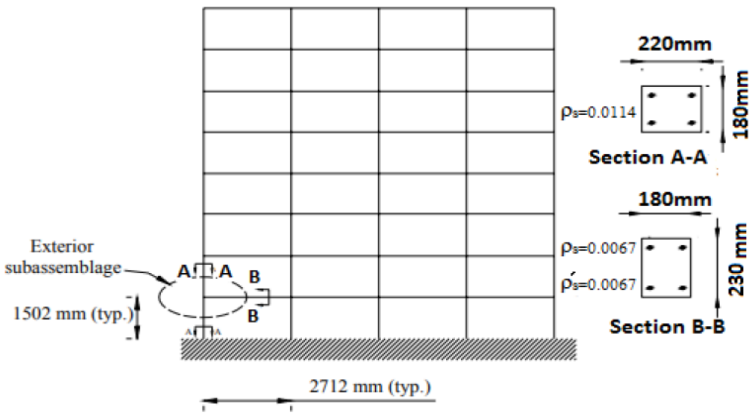

Fig. 1 Typical exterior beam-column joint

This is to ensure that penetration of plasticity to the joint core will not occur, as this may trigger a brittle failure within the core (Thomas and Priestley 1992, Chutarat and Aboutaha 2003). The current study focuses on the experimental and numerical analyses on strengthening of RC BCCs using web bonding of FRP composites. The behaviour of RC BCCs reinforced externally with CFRP composite elements under static loading is primarily investigated. This involves wrapping and attaching FRP plies around the connection area, and the influences of thethickness and lengths of CFRP plates is verified. The validity of external reinforcing systems is verified by comparing the experimental results, and non- linear finite element modelling.

This research project comprises two main parts, namely experimental testing and numerical analysis. Experimental testing is very costly and time-consuming. Hence, accurate finite element modeling of the connections is very important for more extensive verification of the test parameters and also to achieve certain results that could not otherwise be observed through experimental testing. This objective can be achieved through accurate modeling by considering parameters like nonlinearity, material geometries (i.e., concrete crushing and cracking, contact interaction) and suitable elements for modeling the interaction between steel and concrete.

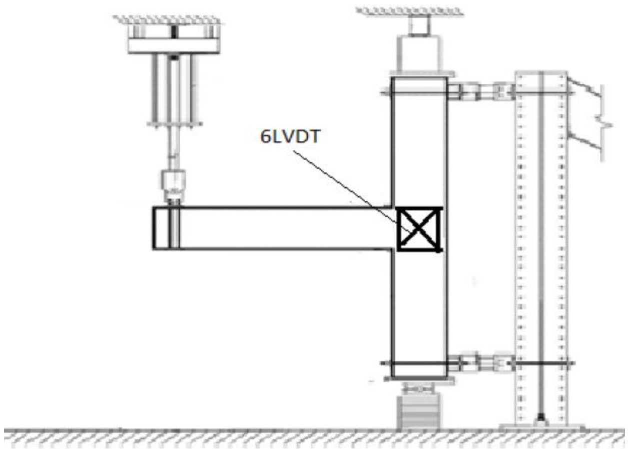

Fig. 2 Exterior beam-column joint sub assemblage

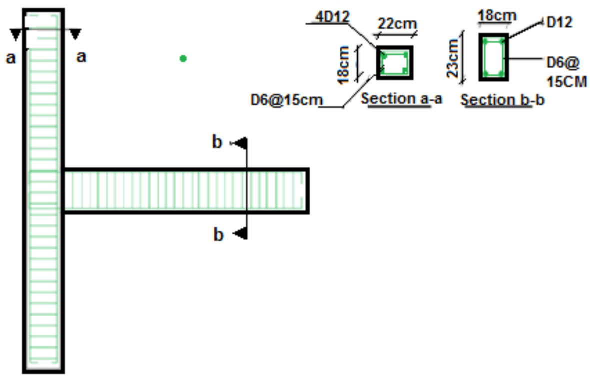

Fig. 3 Geometry of control specimen

2. Experimental test

2.1 Specimens and test setup

An experimental program was conducted to evaluate the performance and behavior of beam-column joint retrofitted with web bonded CFRP composite plates. The specimens were tested by applying both gravity and lateral load on a sub-assembly of exterior reinforced concrete (RC) beam-column joint.

Some tests on some subassemblies using a testing rig were performed by (Mahini and ROUNAGH 2007). The prototype structure was a typical eight-story residential RC building, with details similar to non-ductile RC frames designed (ACI-318-2008). The scaled-down joints were extended to the column mid-height and beam mid-span, corresponding to the infection points of the bending moment diagram under lateral loads. This isolated subassembly represents an external joint in a scaled-down reinforced concrete building (Fig. 1).

The T-shape as an exterior joint was selected for the geometry of the Specimens in the experimental test. A control specimen (non-retrofitted) and a retrofitted specimen with web bonded CFRP plates were tested. Fig. 2 shows a typical test specimen for the experimental test. Test specimens were two 1:2.2 downscale models of the

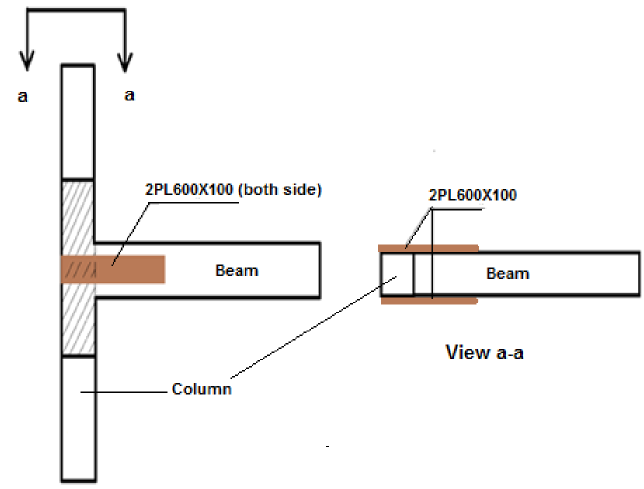

Fig. 4 FRP configuration of RCS5

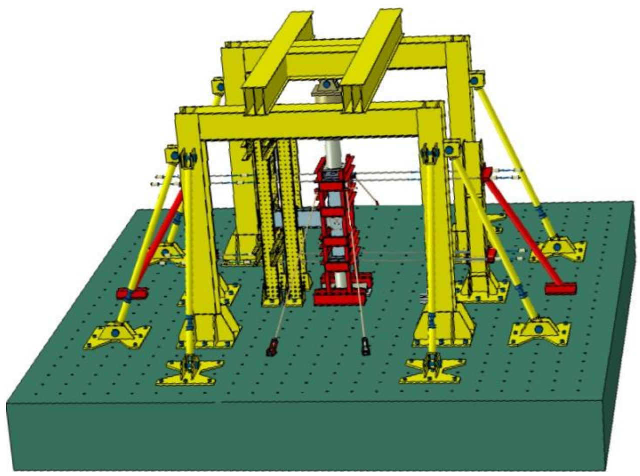

Fig. 5 Schematic view of the test setup

prototype. Both joints consisted of 180 mm wide and 230 mm deep beams with 220 mm × 180 mm columns. Reinforcement consisted of R6 (D = 6. mm) ties of yield Stress (f_y) equal to 400 MPa and Ultimate Stress (f_u) equal to 600 MPa , N12 (D = 12 mm) main bars of yield Stress(f_y) equal to 500 MPa and ultimate Stress (f_u) equal to 700 MPa, and yield strain equal to 0.003 mm/mm. Carbon fibre reinforced plastic (CFRP) sheets that were used in the experiments were unidirectional with an ultimate stress of 3500 MPa, ultimate strain of 0.017 mm/mm and a constantmodulus of 210 GPa. The concrete had a compressive strength of 40.1 and 39.2 MPa for plain (RCS1) and retrofitted specimen (RCS5) respectively.

The column was wrapped with CFRP on both sides as well as around the back of the beam. The ends of CFRP plate also were wrapped in order to provide FRP anchorage. Specimen's geometry and FRP configuration are shown in Figs. 3 and 4.

2.2 Description of test setup

The specimens were placed in the test setup such that the column longitudinal axis was vertical and the beam longitudinal axis was horizontal direction (Fig. 5).

A rigid steel column cap was used for the top and bottom of the column to uniformly distribute the applied axial load over the concrete. In making the pinned connection for the column ends, a steel roller was welded to the caps. The column caps were supported in the plane of loading using high strength threaded rods, which, from one side, were attached to the strong support, and on the other side were connected to the caps by special swivels. The swivels allowed full rotation of the specimens in the plane of loading. The threaded rods were pre-loaded during the installation of the specimens to prevent lateral movement of the specimens. The column caps were also supported using a strong frame, which was restrained to the strong floor by lateral threaded rods. Special bearings were used to connect the caps to the frame. This frame was used to prevent out of plan lateral displacement of the column and also to restrain the 2000 kN actuator. The beam was restrained in the lateral direction to prevent lateral tensional buckling from taking place. In the first step of loading; the column was loaded with a constant axial load, which was applied using a 2,000 kN hydraulic actuator to represent the reaction from the upper floors and the corresponding ratio was about 20% of the column capacity (0.20Agfc) practical range in real frame buildings (Hwang and Lee 1999, 2002, Hui and Irawan 2001, Mahini and ROUNAGH 2007). The axial load value was kept constant during the rest of the test. In step two, one vertical load were applied at the beam end to simulate the deformed shape of a similar connection in a building subjected to lateral loads. The beam load was applied using a 500 kN actuators. Displacement control was used to apply monotonic deflection in small increments until failure of the specimens.

The applied loads and vertical displacement of the column tops and beam end were measured using load cells which were attached to the related actuators. Nine linear voltage displacement transducers (LVDT) were used to monitor displacement of the specimens as well (Fig. 6). All the readings from the instrumentation were recorded

Fig. 6 Installed LVDT on the column

Fig. 7 RCS1 specimen after failure

automatically using a data logger system, which was controlled by a personal computer.

3. Results and discussions

3.1 General

In the control specimen (RCS1), flexural cracking of the beam section subjected to maximum bending moment initially appeared at a beam tip load of 6.7 kN. Cracks were detected simultaneously beside the beam close to the column. The onset of diagonal cracks in the joint area took place at a beam tip load of 10 kN. Additional cracks in the joint area appeared thereafter as loading progressed but remained within a very fine width throughout the test. The beam's longitudinal steel yielded at an average beam tip load of 12 kN and the corresponding average yield displacement (D_y) was 34 mm. Subsequently, the beam cracked extensively along a distance shorter than its depth from the column face. Finally, wide cracks developed in the hinge area at a beam tip load of 12.8 kN and the test was stopped as the beam capacity dropped substantially. Fig. 7 shows the specimen RCS1after failure.

Table 1 The ultimate load and ductility factor of specimens

Specimen	Ultimate load (kN)	Ductility factor
RCS1	12.8	1.91
RCS5	21.86	3.9

During the test, a data logger recorded the load and corresponding displacement. Fig. 8 displays the load variations against displacement for both specimens. The presence of CFRP reinforcement affected the ultimate load and ductility factor of the specimens.

The first bending crack started at F = 5.5 kN and the shear stress increased, but on account of the CFRP plates, shear cracking was controlled. At higher loads, new cracks formed paralleled to the beam. According to strain gauge data, the top beam rebars yielded. The location where a plastic hinge formed was not sufficiently far from the column; therefore, by choosing suitable CFRP plate lengths and optimizing the CFRP thickness, it is possible to predict a more appropriate point on the beam for plastic hinge formation. The CFRP plates helped control the SHEAR stress while the shear resistance of specimen RCS5 rose. The maximum stress of the longitudinal rebar reduced and the specimen became more ductile.

3.2 Ductility factor and ultimate load

When the data logger recorded the first yield that occurred to any of the steel reinforcement rebars, the corresponding displacement (D_y) was measured. The data logger recorded the load and corresponding displacement. The ultimate load has increased 71% for RCS5. The data logger also recorded displacement corresponding to ultimate load (D_u). D_y and D_u were used to calculate the experimental ductility factor (μ). The ductility factor is calculated with Eq. (1) and presented in Table 1.

$$\mu = D_u/D_y \tag{1}$$

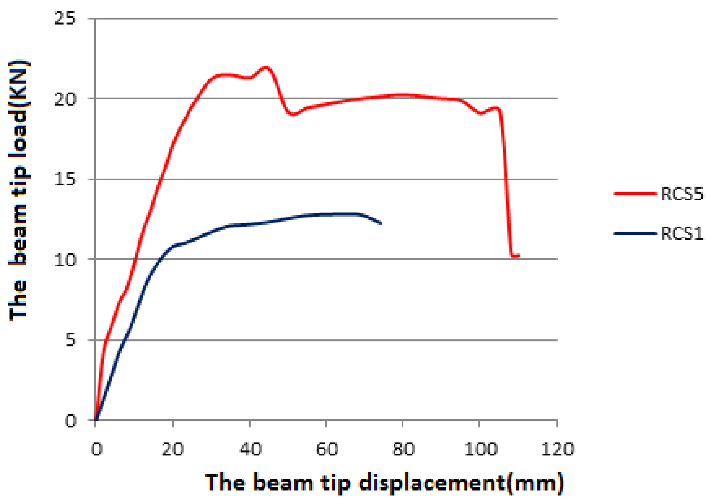

Fig. 8 Load variations against displacement for both specimens RCS1 and RCS5

4. Numerical program

ABAQUS software with its unique features is one of the most powerful applications for reinforced concrete finite element modeling. Owing to the software's ability to model rebars inside concrete such that their behavior matches reality to a great extent, it is feasible to monitor the rebars' behavior details.

4.1 Numerical models

In the models, the damage plasticity for concrete cracking was defined for the specimens. The concrete damage plasticity model presumes a non-associated potential plastic flow. The material dilation angle (Ψ) and eccentricity (Ɛ) were taken as 25° and 0.1, respectively. The ratio of biaxial compressive strength to uniaxial compressive strength ($\frac{f_{b0}}{f_{c0}}$) was taken as 1.16. An eight-node solid element (C3D8R) was used to model the concrete core.

The longitudinal and transverse steel reinforcement rebars were incorporated in the FE model as an elastic-plastic material using a bilinear stress-strain curve. The stress-strain curve slope in the plastic stage was assumed to be about 1% of the modulus of elasticity for steel. The truss element (T3D2) was applied in modeling the longitudinal reinforcing bar and transverse in the specimens.

The unidirectional laminate properties were incorporated in the model as an orthotropic material. The CFRP laminate mechanical properties are defined in the elastic laminate option. The following parameters were entered in the FE model:

(1) Laminate module along and perpendicular to the fibers (E11 and E22).
(2) Laminate shear modulus in the three orthogonal directions (G12, G13, and G23).
(3) Laminate Poisson's ratio (ν12) = 0.3.

The renowned failure index, i.e., Tsai-Wu criterion, was applied to define the failure criteria of the FE analysis model (Tsai and Wu 1971). The fiber reinforcement polymer (FRP) composite laminate was modeled using four node shell elements. The shell element in the FE analysis model is called S4R.

A tie constraint was used to connect the shell element to the concrete solid element. Reinforcement rebar elements were connected to the surrounding concrete regions using an embedded element option. In order to obtain accurate FE modeling results, all elements in the model were purposely assigned the same mesh size to ensure that every two different materials shared the same node. The type of mesh selected in the model was structured. The mesh elements for concrete, rebar and CFRP laminate were 3D solid, 2D truss, and shell, respectively. Two steps similar to the test specimen loading were considered for the loading in finite element analysis. First, axial load was applied on some nodes at the column top. The nodes were located on the line perpendicular to the main specimen plan. The load was kept constant until the end of analysis. The value of the axial load was the same as the axial load applied during the test. Second, vertical velocity loading was applied to the beam end.

4.2 Verification

The laboratory results for the reinforced and prototype samples are compared, and the impact of CFRP reinforcement on the sample's capacity and ductility is examined. Subsequently, samples RCS1 and RCS5 are modeled and analyzed. The numerical results are controlled with the experimental data (Fig. 9). Since it is possible to control various parameters for all components, the samples' details are studied in the numerical analysis, which is simpler and less expensive than lab analysis. Therefore, different models are produced with various CFRP plate lengths and thicknesses. Numerical analysis is then applied to investigate the effect of reinforcing layer length and thickness in different configurations.

4.3 The effect of CFRP plate length and thickness on plastic hinge relocation

One of the main goals of this research was to determine the appropriate length and thickness of CFRP plates in order to improve the beam-column concrete connections. In this section, sample RCS5 with CFRP reinforcement panels of different lengths and thicknesses is evaluated and the effect of changes in CFRP plate length and thickness on the plastic hinge transfer is evaluated. The width of all plates

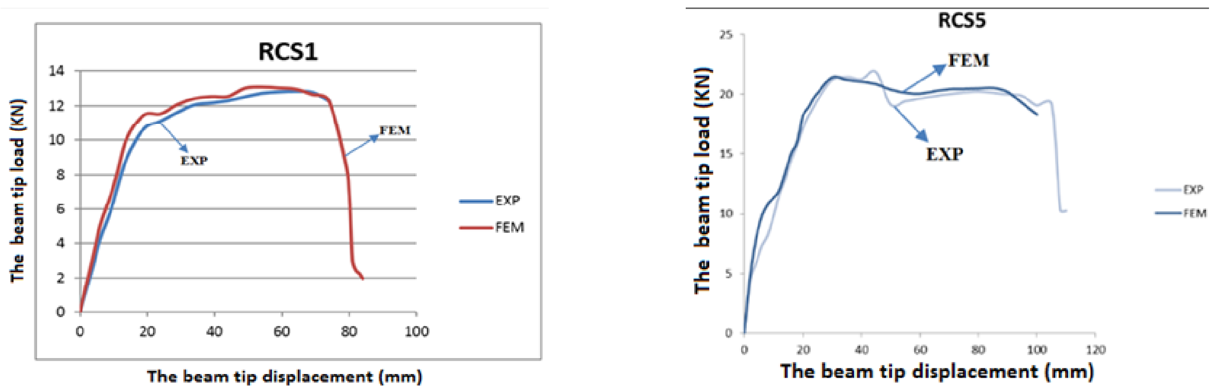

Fig. 9 Verification of numerical results versus experimental results

Table 2 Specification of web bonded sample with 1 mm thickness plates

Sample	Length (cm)	Width (cm)	Thickness (mm)
RCS5L30T10	30	10	1
RCS5L40T10	40	10	1
RCS5L50T10	50	10	1
RCS5L60T10	60	10	1
RCS5L70T10	70	10	1
RCS5L80T10	80	10	1

was fixed at 10 cm. Plates with thicknesses of 1, 1.2, 1.4, 1.6 and 1.8 mm was modeled, and for each thickness, lengths of 30, 40, 50, 60, 70, and 80 cm were considered. Moreover, for plates with thicknesses of 2, 2.2 and 2.4 mm, lengths of 70 and 80 cm were modeled.

4.3.1 Sample RCS5 reinforced with 1 mm thick plates bonded on the beam web

First, six samples 10 cm wide and 1 mm thick, all with two reinforcement CFRP plates on both sides of the beam web were modeled. Different lengths of 30, 40, 50, 60, 70 and 80 cm were considered, and the samples were denoted as RCS5L30T10, RCS5L40T10, RCS5L50T10, RCS5L60T10, RCS5L70T10 and RCS5L80T10, respecti- vely. The specifications of all samples are summarized in Table 2.

Modeling was done similar to previous sections and all dimensions and sizes were considered fixed except for the reinforcement plate lengths. The boundary conditions and loading were also as mentioned. The strain graphs of the top longitudinal beam rebars for these six samples are shown in Figs. 10(a-f).

As seen in Fig. 1(a), for the sample with a plate 1 mm thick, using a length of 30 cm caused maximum strain for both longitudinal rebars (R1, R2) to occur at the end of the CFRP layer. However, given the fact that the 30 cm length started from the back of the column, the end of the CFRP plate was only 8 cm from the beam-column connection point, which is not a reliable distance.

According to Fig. 10(b), the 1 mm thick and 40cm long plate had a more suitable condition than other lengths. This caused maximum strain of the two longitudinal reinforce- ments (R1, R2) to occur at the end of the CFRP plate, indicating that plastic hinge relocation was somewhat successful.

However, as shown in Fig. 10(c), the increase in CFRP plate length up to 50 cm did not help improve the plastic hinge movement.

Fig. 10(d) also indicates that for a CFRP plate of the same thickness and 60cm long, the difference between the

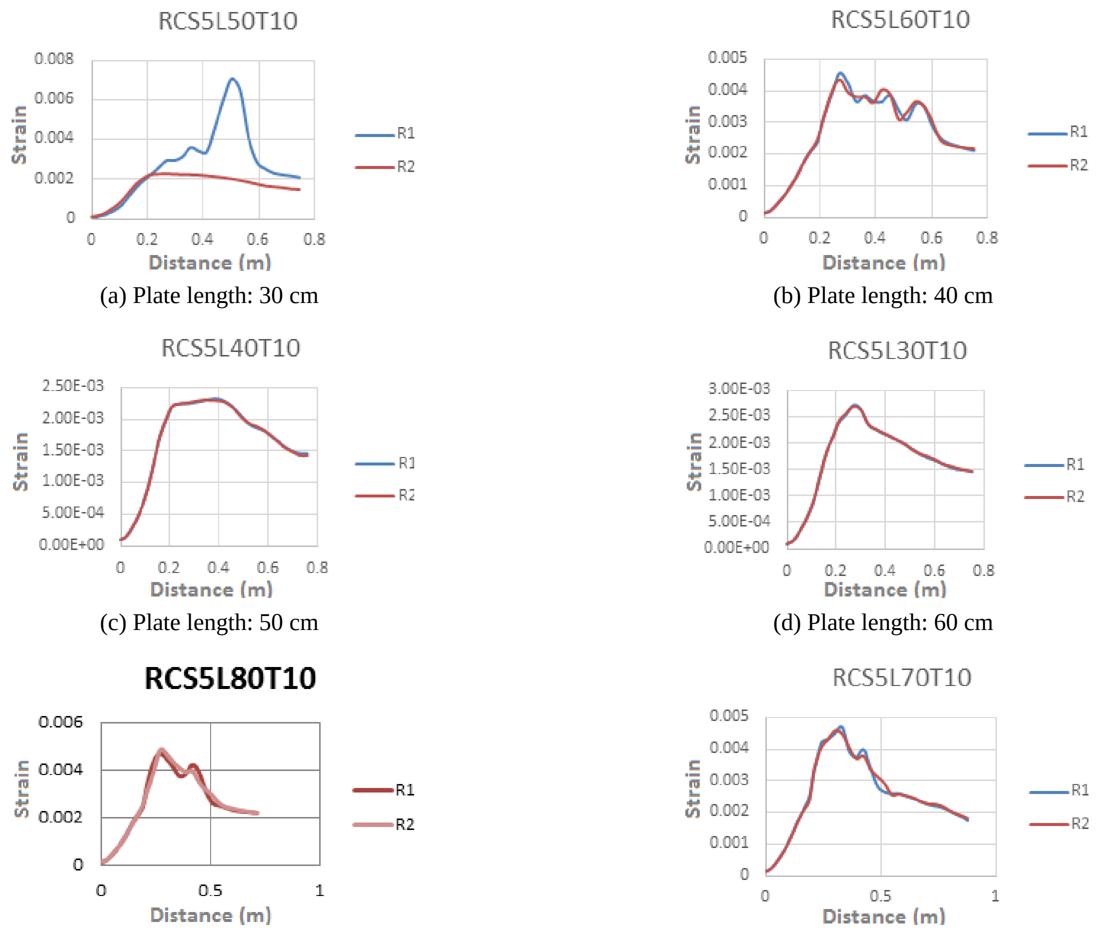

(a) Plate length: 30 cm
(b) Plate length: 40 cm
(c) Plate length: 50 cm
(d) Plate length: 60 cm
(e) Plate length: 70 cm
(f) Plate length: 80 cm

Fig. 10 Steel strain distribution diagram for reinforced specimen with web bonded plates 1 mm in thickness strain at the end of the CFRP and beside the column decreased. This decrease continued until the 1 mm thick CFRP length increased to 70 and 80 cm (Fig. 10(e), (f)), when the maximum strain of all tensile longitudinal rebars occurred at the column. Apparently, the plastic hinge relocation was completely unsuccessful at these lengths.

4.3.2 Sample RCS5 reinforced with 1.2 mm thick plates bonded on the beam web

Sample RCS5 was modeled once again. This time, the thickness of the web reinforcement plate was increased to 1.2 mm. The sample was analyzed for CFRP reinforcement plates with lengths of 30, 40, 50, 60, 70 and 80 cm. Details of the modeled samples are given in Table 2.

At the end of each analysis, a strain distribution diagram was drawn for the upper longitudinal rebars depending on the distance between points and the column.

4.3.3 Sample RCS5 reinforced with 1.4 mm thick plates bonded on the beam web

The same samples from the previous sections with 1.4 mm thick web CFRP reinforcement plates are analyzed. Details of these samples are given in Table 3.

4.3.4 Sample RCS5 reinforced with 1.6 mm thick plates bonded on the beam web

These groups of samples were modeled using 1.6 mm thick web bonded CFRP plates. Details of these samples are provided in Table 4.

4.3.5 Sample RCS5 reinforced with 1.8 mm thick plates bonded on the beam web

In this section, the web bonded CFRP reinforcement plate thickness was increased to 1.8 mm. Table 5 presents the details of the six samples analyzed in this section.

4.3.6 Sample RCS5 reinforced with 2, 2.2 and 2.4 mm thick web bonded plates

An attempt was made to find out whether increasing the plate thickness would produce favorable results for the samples reinforced with 70 and 80 cm long CFRP plates. To this end, the RCS5 sample with 10 cm wide and 70 and 80 cm long reinforcement plates on both sides of the web was analyzed by increasing the plate thickness to 2 mm, 2.2 mm, and 2.4 mm. Table 6 provides details of the six samples analyzed in this section.

However, as seen in Figs. 11 to 13 plastic hinge transfer did not occur in any of these samples. Thus, it can be concluded that the effect of increasing the reinforcing plate length limited the plastic joint movement. The increase in length was limited to about twice the beam height.

In the first category, where CFRP plates were installed on both sides of the beam web, 1 mm thick reinforcing plates with lengths of 30, 40, 50, 60, 70 and 80 cm were analyzed. The results showed that with 30 and 40 cm long plates, the plastic hinge was relocated to the end of the CFRP plates. However, other lengths did not succeed in relocating the plastic hinge. In the next step, the CFRP plate thickness was increased to 1.2 mm and results similar to the first stage were obtained. The status of the sample with a 40 cm long reinforcement plate improved slightly. However, the lengths of 50, 60, 70 and 80 cm did not fulfill the expected plastic hinge transfer. Subsequently, the CFRP plate thickness was increased to 1.4 mm. This time, it was observed that in addition to the lengths of 30 and 40 cm, the 50 cm long plate was successful in transferring the plastic hinge. Lengths greater than 50 cm did not perform well. With increasing the plate thickness in the next steps, it appeared that the 60 cm length and 1.8 mm thickness also

Table 3 Specifications of samples with 1.2 mm thick web bonded plates

Sample	Length (cm)	Width (cm)	Thickness (mm)
RCS5L30T12	30	10	1.2
RCS5L40T12	40	10	1.2
RCS5L50T12	50	10	1.2
RCS5L60T12	60	10	1.2
RCS5L70T12	70	10	1.2
RCS5L80T12	80	10	1.2

Table 4 Specifications of samples with 1.4 mm thick web bonded plates

Sample	Length (cm)	Width (cm)	Thickness (mm)
RCS5L30T14	30	10	1.4
RCS5L40T14	40	10	1.4
RCS5L50T14	50	10	1.4
RCS5L60T14	60	10	1.4
RCS5L70T14	70	10	1.4
RCS5L80T14	80	10	1.4

Table 5 Specifications of samples with 1.6 mm thick web bonded plates

Sample	Length (cm)	Width (cm)	Thickness (mm)
RCS5L30T16	30	10	1.6
RCS5L40T16	40	10	1.6
RCS5L50T16	50	10	1.6
RCS5L60T16	60	10	1.6
RCS5L70T16	70	10	1.6
RCS5L80T16	80	10	1.6

Table 6 Specifications of samples with 1.8 mm thick web bonded plates

Sample	Length (cm)	Width (cm)	Thickness (mm)
RCS5L30T18	30	10	1.8
RCS5L40T18	40	10	1.8
RCS5L50T18	50	10	1.8
RCS5L60T18	60	10	1.8
RCS5L70T18	70	10	1.8
RCS5L80T18	80	10	1.8

functioned suitably. However, 1.8 mm thick and 70 and 80 cm long plates were not suitable. Next, suitable thicknesses for the 70 and 80 cm long reinforcement plates were evaluated. Here, the samples analyzed contained 2, 2.2 and 2.4 mm thick for 70 and 80 cm long reinforcement plates. The results revealed that none of these patterns were effective on shifting the plastic hinge. Thus, it can be concluded that despite the ability to increase the effective length of the CFRP plates by increasing their thickness to create a plastic hinge at the end of the CFRP plates, there were some limitations. As such, it was not possible to increase the reinforcement plate length, and thereby the plastic hinge distance from the column as much as anticipated. It was deduced that the maximum effective CFRP plate length, or in other words the distance from the plastic joint formation on the column, can be considered to be about twice the height of the beam.

Table 7 Specifications of samples with 2, 2.2 and 2.4 mm thick web bonded plates

Sample	Length (cm)	Width (cm)	Thickness (mm)
RCS5L70T20	70	10	2.0
RCS5L80T20	80	10	2.0
RCS5L70T22	70	10	2.2
RCS5L80T22	80	10	2.2
RCS5L70T24	70	10	2.4
RCS5L80T24	80	10	2.4

5. Conclusions

The purpose of this research was to evaluate the ability of CFRP reinforcement to enhance strength and ductility. Meanwhile, the aim of this study was to prevent plastic hinge formation at the column face in the exterior beam-column joint by using an advanced CFRP laminate. As the results:

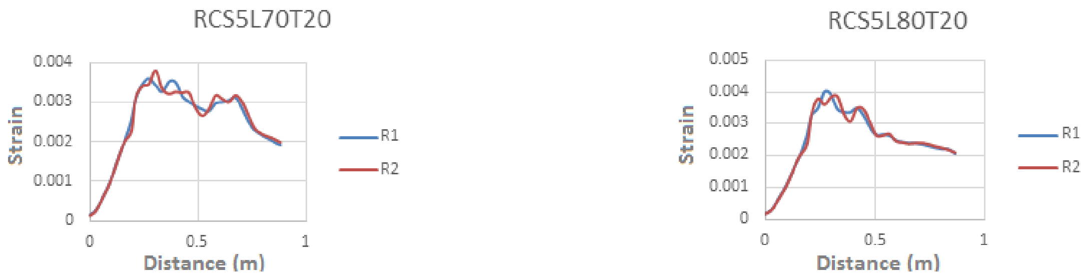

(a) Plate length: 70 cm (b) Plate length: 80 cm

Fig. 11 Steel strain distribution diagrams for specimens reinforced with 2 mm thick web bonded plates

(a) Plate length: 70 cm (b) Plate length: 80 cm

Fig. 12 Steel strain distribution diagrams for specimens reinforced with 2.2 mm thick web bonded plates

(a) Plate length: 70 cm (b) Plate length: 80 cm

Fig. 13 Steel strain distribution diagrams for specimens reinforced with 2.4 mm thick web bonded plates

(1) In the experimental program, two scaled-down RC exterior joints were tested under moderately monotonic loads. One specimen was the control while the other specimens were strengthened specimen with web bonded CFRP plates. Applying the CFRP reinforcement increased the load capacity of the beam-column connections. The ductility factor of retrofitted sample (RCS5) increased (almost %100).

(2) The control specimen and retrofitted joint were simulated in Finite Element (FE) modeling software (ABAQUS) and then analyzed. The numerical analysis results seemed to be in acceptable compliance with the experimental results, except for a slight difference in the results from the actual values of about 1% to 3%. Following numerical analysis with ABAQUS, the stress and strain contours were examined and compared with experimental observations, and the results were recorded in a data logger. The behavior of the numerical specimens was completely consistent with that of the experimental specimens. The locations of cracking and concrete damage as well as plastic hinge in the rebars were in good agreement in both numerical and experimental methods.

(3) After numerical method validation, several CFRP-reinforced samples with different plate lengths and thicknesses were analyzed for their ability to relocate the plastic hinge away from the column face.

The results demonstrated that the effective length of a CFRP plate to relocate the plastic hinge is dependent on its thickness. It was found that by increasing the reinforcing plate thickness, the plate effective length on plastic hinge transfer increased. However, this increase is limited and excessive thickening may have negative effects. The optimum effective CFRP plate length can be considered a distance about twice the height of the beam from behind the column.

References

ACI-318-2008 318 (2008), Building Code Requirements for Structural Concrete (ACI 318-08) and Commentary (ACI 318R-08); American Concrete Institute (ACI), Detroit, MI, USA.

Allahvirdizadeh, R., Rashetnia, R., Dousti, A. and Shekarchi, M. (2011), “Application of polymer concrete in repair of concrete structures: A literature review”, *Concrete Solutions*, 435-444.

Andalib, Z., Kafi, M.A., Kheyroddin, A. and Bazzaz, M. (2014), “Experimental investigation of the ductility and performance of steel rings constructed from plates”, *J. Constr. Steel Res.*, **103**, 77-88.

Aslam, M., Shafigh, P., Jumaat, M.Z. and Shah, S.N.R. (2015), “Strengthening of RC beams using prestressed fiber reinforced polymers–A review”, *Constr. Build. Mater.*, **82**, 235-256.

Chutarat, N. and Aboutaha, R.S. (2003), “Cyclic Response of Exterior Reinforced Concrete Beam-Column Joints Reinforced with Headed Bars – Experimental Investigation”, *ACI Structural Journal*, **100**(2).

Daie, M., Jalali, A., Suhatril, M., Shariati, M., Khanouki, M.A., Shariati, A. and Kazemi-Arbat, P. (2011), “A new finite element investigation on pre-bent steel strips as damper for vibration control”, *Int. J. Phys. Sci.*, **6**(36), 8044-8050.

Daly, A. and Witarnawan, W. (1997), “Strengthening of bridges using external post-tensioning”, Paper PA3307/97; Transportation Research Laboratory, Berkshire, UK.

Engindeniz, M., Kahn, L.F. and Abdul-Hamid, Z. (2005), “Repair and strengthening of reinforced concrete beam-column joints: State of the art”, *ACI Struct. J.*, **102**(2).

Hadi, M.N. and Tran, T.M. (2016), “Seismic rehabilitation of reinforced concrete beam–column joints by bonding with concrete covers and wrapping with FRP composites”, *Mater. Struct.*, **49**(1-2), 467-485.

Hamidian, M., Shariati, A., Khanouki, M.A., Sinaei, H., Toghroli, A. and Nouri, K. (2012), “Application of Schmidt rebound hammer and ultrasonic pulse velocity techniques for structural health monitoring”, *Sci. Res. Essays*, **7**(21), 1997-2001.

Heydari, A. and Shariati, M. (2018), “Buckling analysis of tapered BDFGM nano-beam under variable axial compression resting on elastic medium”, *Struct. Eng. Mech., Int. J.*, **66**(6), 737-748.

Hui, Y. and Irawan, P. (2001), “Behaviour of full-scale lightly reinforced concrete beam-column joints”, Civil Engineering Research, Nanyang Technological University, Singapore, pp. 44-45.

Hwang, S.-J. and Lee, H.-J. (1999), “Analytical model for predicting shear strengths of exterior reinforced concrete beam-column joints for seismic resistance”, *ACI Struct. J.*, **96**(5).

Hwang, S.-J. and Lee, H.-J. (2002), “Strength prediction for discontinuity regions by softened strut-and-tie model”, *J. Struct. Eng.*, **128**(12), 1519-1526.

Jalali, A., Daie, M., Nazhadan, S.V.M., Kazemi-Arbat, P. and Shariati, M. (2012), “Seismic performance of structures with pre-bent strips as a damper”, *Int. J. Phys. Sci.*, **7**(26), 4061-4072.

Joshaghani, A. (2017), “The effect of trass and fly ash in minimizing alkali-carbonate reaction in concrete”, *Constr. Build. Mater.*, **150**, 583-590.

Joshi, S.G., Londhe, S.N. and Kwatra, N. (2014), “Determination of natural periods of vibration using genetic programming”, *Earthq. Struct., Int. J.*, **6**(2), 201-216.

Khanouki, A., Ramli Sulong, M.M. and Shariati, N.H. (2010), “Investigation of seismic behaviour of composite structures with concrete filled square steel tubular (CFSST) column by push-over and time-history analyses”, *Proceedings of the 4th International Conference on Steel & Composite Structures*, Sydney, Australia, July.

Khanouki, A., Mehdi, M., Ramli Sulong, N.H. and Shariati, M. (2011), “Behavior of through Beam Connections Composed of CFSST Columns and Steel Beams by Finite Element Studying”, *Adv. Mater. Res.*, **168**, 2329-2333.

Khorami, M., Alvansazyazdi, M., Shariati, M., Zandi, Y., Jalali, A. and Tahir, M. (2017), “Seismic performance evaluation of buckling restrained braced frames (BRBF) using incremental nonlinear dynamic analysis method (IDA)”, *Earthq. Struct., Int. J.*, **13**(6), 531-538.

Liu, Y., Malaga-Chuquitaype, C. and Elghazouli, A.Y. (2014), “Behaviour of open beam-to-tubular column angle connections under combined loading conditions”, *Steel Compos. Struct., Int. J.*, **16**(2), 157-185.

Mahini, S. and ROUNAGH, H. (2007), “A new method for improving ductility in existing RC ordinary moment resisting frames using FRPs.”

McCormac, J.C. and Brown, R.H. (2015), *Design of Reinforced Concrete*, John Wiley & Sons.

Mohammadhassani, M., Suhatril, M., Shariati, M. and Ghanbari, F. (2013a), “Ductility and strength assessment of HSC beams with varying of tensile reinforcement ratios", *Struct. Eng. Mech.*, *Int. J.*, **48**(6), 833-848.

Mohammadhassani, M., Nezamabadi-Pour, H., Suhatril, M. and Shariati, M. (2013b), "Identification of a suitable ANN architecture in predicting strain in tie section of concrete deep beams", *Struct. Eng. Mech.*, *Int. J.*, **46**(6), 853-868.

Mohammadhassani, M., Akib, S., Shariati, M., Suhatril, M. and Khanouki, M.A. (2014a), "An experimental study on the failure modes of high strength concrete beams with particular references to variation of the tensile reinforcement ratio", *Eng. Fail. Anal.*, **41**, 73-80.

Mohammadhassani, M., Nezamabadi-Pour, H., Suhatril, M. and Shariati, M. (2014b), "An evolutionary fuzzy modelling approach and comparison of different methods for shear strength prediction of high-strength concrete beams without stirrups", *Smart Struct. Syst.*, *Int. J.*, **14**(5), 785-809.

Momenzadeh, S., Seker, O., Faytarouni, M. and Shen, J. (2017), "Seismic performance of all-steel buckling-controlled braces with various cross-sections", *J. Constr. Steel Res.*, **139**, 44-61.

Nordin, H. (2005), "Strengthening structures with externally prestressed tendons: literature review."

Shafaei, S., Ayazi, A. and Farahbod, F. (2016), "The effect of concrete panel thickness upon composite steel plate shear walls", *J. Constr. Steel Res.*, **117**, 81-90.

Shahabi, S.E.M., Sulong, N.H., Shariati, M., Mohammadhassani, M. and Shah, S.N.R. (2016), "Numerical analysis of channel connectors under fire and a comparison of performance with different types of shear connectors subjected to fire", *Steel Compos. Struct.*, *Int. J.*, **20**(3), 651-669.

Shariat, M., Shariati, M., Madadi, A. and Wakil, K. (2018), "Computational Lagrangian Multiplier Method using optimization and sensitivity analysis of rectangular reinforced concrete beams", *Steel Compos. Struct.*, *Int. J.*, **29**(2), 243-256.

Shariati, M. (2008), Assessment Building Using None-destructive Test Techniques (ultra Sonic Pulse Velocity and Schmidt Rebound Hammer), Universiti Putra Malaysia.

Sinaei, H., Jumaat, M.Z. and Shariati, M. (2011), "Numerical investigation on exterior reinforced concrete Beam-Column joint strengthened by composite fiber reinforced polymer (CFRP)", *Int. J. Phys. Sci.*, **6**(28), 6572-6579.

Sinaei, H., Shariati, M., Abna, A.H., Aghaei, M. and Shariati, A. (2012), "Evaluation of reinforced concrete beam behaviour using finite element analysis by ABAQUS", *Sci. Res. Essays*, **7**(21), 2002-2009.

Tang, W.C., Balendran, R.V., Nadeem, A. and Leung, H.Y. (2006), "Flexural strengthening of reinforced lightweight polystyrene aggregate concrete beams with near-surface mounted GFRP bars", *Build. Environ.*, **41**(10), 1381-1393.

Thomas, P. and Priestley, M. (1992), *Seismic Design of Reinforced Concrete and Masonry Buildings*, New York Wiley-Interscience.

Tsai, S.W. and Wu, E.M. (1971), "A general theory of strength for anisotropic materials", *J. Compos. Mater.*, **5**(1), 58-80.

Zandi, Y., Shariati, M., Marto, A., Wei, X., Karaca, Z., Dao, D., Toghroli, A., Hashemi, M.H., Sedghi, Y., Wakil, K. and Khorami, M. (2018), "Computational investigation of the comparative analysis of cylindrical barns subjected to earthquake", *Steel Compos. Struct.*, *Int. J.*, **28**(4), 439-447.

CC